Cancer Cell
Article

miR-30b/30d Regulation of GalNAc Transferases Enhances Invasion and Immunosuppression during Metastasis

Avital Gaziel-Sovran,[1,2] Miguel F. Segura,[1,2] Raffaella Di Micco,[1,2] Mary K. Collins,[1] Douglas Hanniford,[1,2] Eleazar Vega-Saenz de Miera,[2,3] John F. Rakus,[6] John F. Dankert,[1,2] Shulian Shang,[4] Robert S. Kerbel,[8] Nina Bhardwaj,[1,2,5] Yongzhao Shao,[4] Farbod Darvishian,[1,2] Jiri Zavadil,[1,6] Adrian Erlebacher,[1] Lara K. Mahal,[7] Iman Osman,[2,3,5] and Eva Hernando[1,2,*]
[1]Department of Pathology
[2]Interdisciplinary Melanoma Cooperative Group
[3]Department of Dermatology
[4]Department of Environmental Medicine
[5]Department of Medicine
[6]NYU Center for Health Informatics and Bioinformatics
New York University Medical Center, New York, NY 10016, USA
[7]Department of Chemistry, New York University, New York, NY 10003, USA
[8]Department of Medical Biophysics, University of Toronto, Toronto, ON M4N 3M5, Canada
*Correspondence: eva.hernando@med.nyu.edu
DOI 10.1016/j.ccr.2011.05.027

SUMMARY

To metastasize, a tumor cell must acquire abilities such as the capacity to colonize new tissue and evade immune surveillance. Recent evidence suggests that microRNAs can promote the evolution of malignant behaviors by regulating multiple targets. We performed a microRNA analysis of human melanoma, a highly invasive cancer, and found that miR-30b/30d upregulation correlates with stage, metastatic potential, shorter time to recurrence, and reduced overall survival. Ectopic expression of miR-30b/30d promoted the metastatic behavior of melanoma cells by directly targeting the GalNAc transferase GALNT7, resulted in increased synthesis of the immunosuppressive cytokine IL-10, and reduced immune cell activation and recruitment. These data support a key role of miR-30b/30d and GalNAc transferases in metastasis, by simultaneously promoting cellular invasion and immunosuppression.

INTRODUCTION

Far more attention has been given to the process of malignant transformation than to metastasis, yet it is the spread of transformed cells that accounts for 90% of deaths from solid tumors (Gupta and Massagué, 2006). The capacity of a tumor cell to metastasize depends upon its ability to escape the primary tumor, intravasate into circulation, survive transit, extravasate into distant tissue, and colonize it, while evading immune surveillance and promoting various changes to the local tissue environment (Gupta and Massagué, 2006). The conventional view of tumor progression assumed that malignant cells evolve these aggressive functions over time, but we are beginning to appreciate that metastatic traits may be acquired earlier rather than later in oncogenesis (Gupta et al., 2005; Scheel et al., 2007; Talmadge, 2007).

Accumulating evidence suggests that alterations in microRNA (miRNA) expression might prove crucial in promoting

Significance

microRNAs are emerging as key contributors to tumor metastasis because of their ability to regulate multiple targets and thereby alter several functions simultaneously. We found a miRNA cluster that promotes metastasis by concurrently enhancing invasive capabilities of melanoma cells and suppressing immune surveillance mechanisms, allowing the tumor cells to migrate and invade foreign tissue. Both these effects of *miR-30b/30d* are mediated by direct suppression of GalNAc transferases. Aberrant glycosylation has previously been connected to tumor progression, but the underlying molecular mechanisms and their impact on specific cellular pathways are poorly understood. Our work places the control of glycosylation as a molecular link between tumor cell migration and immune evasion, two processes that act synergistically during metastasis.

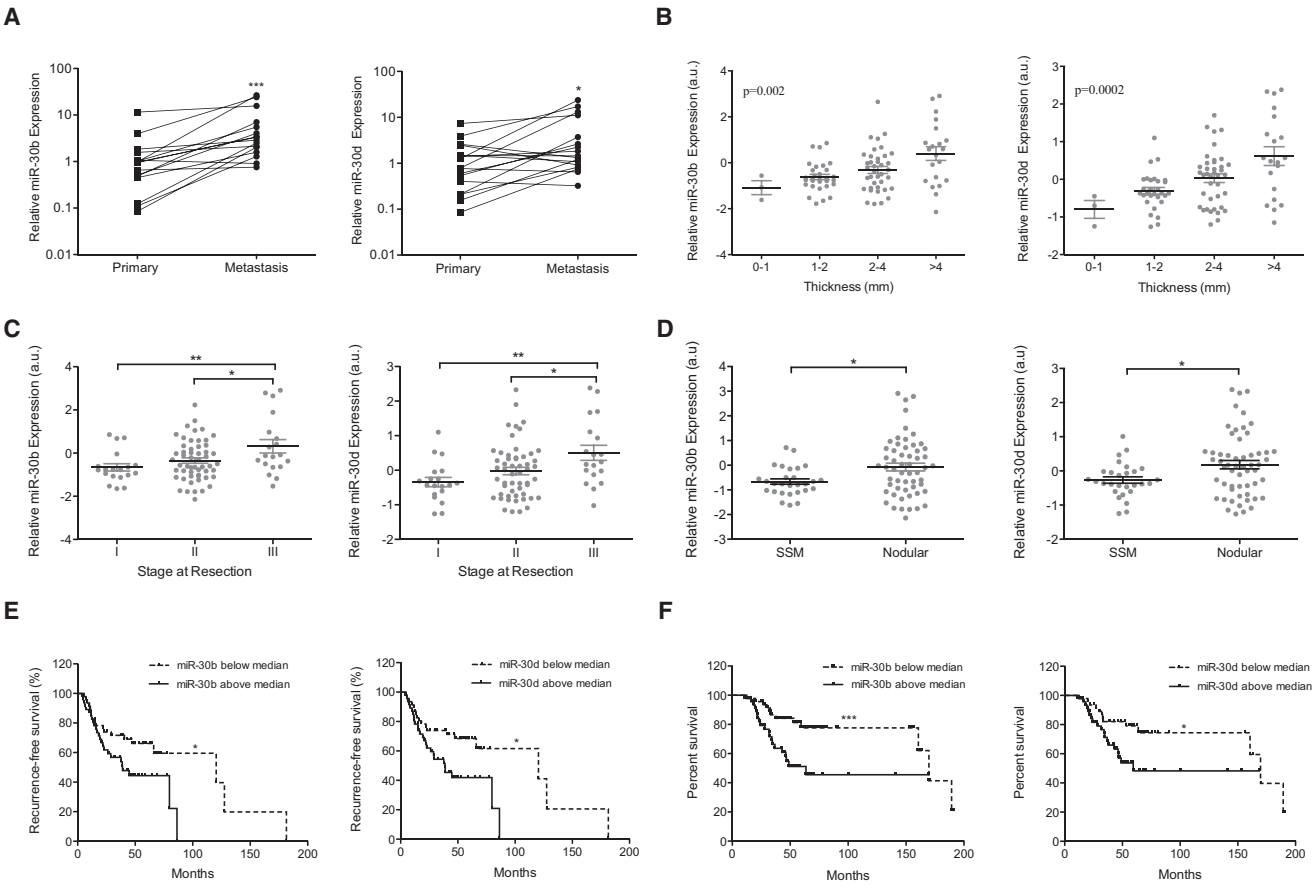

Figure 1. High *miR-30b* and *miR-30d* Levels Are Associated with Metastatic Behavior, Shorter Time to Recurrence, and Lower Overall Survival in Melanoma

(A) Increased relative levels of *miR-30b* and *miR-30d* in 17 metastatic cases compared to the levels in their matched primary tumors, as measured by qRT-PCR.
(B and C) *miR-30b* and *miR-30d* normalized array levels in 92 primary cases with (B) increased thickness and (C) increased stage. ANOVA test was applied in (B).
(D) *miR-30b* and *miR-30d* normalized array levels in superficial spreading melanoma (SSM) (n = 28) versus nodular melanoma (n = 56).
(E and F) Curves show shorter time to recurrence (E) and lower overall survival (F; n = 92) in patients with high (above median value) versus low (below median value) *miR-30b/30d* levels. (*p < 0.05; **p < 0.01; ***p < 0.001).
See also Figure S1 and Table S1.

metastasis (Croce and Calin, 2005; Ma et al., 2007, 2010; Tavazoie et al., 2008). This is an intuitively compelling idea because miRNAs have been found to serve important regulatory functions during numerous developmental and pathological processes by altering multiple target genes and, therefore, multiple cellular activities, simultaneously (Gupta and Massagué, 2006). Expression profiling has identified miRNA signatures for a number of tumors that correlate with disease stage and clinical outcome (Calin and Croce, 2006). The extent to which these alterations in miRNA expression actually influence metastasis is difficult to decipher because in many cases the miRNAs exert confounding effects on cell growth and proliferation within the primary tumor (Tavazoie et al., 2008). Given both the importance of metastasis to cancer-associated lethality and our relatively tenuous grasp of how it is executed by tumor cells, we sought to investigate the role of miRNAs in one of the most invasive tumor types, melanoma.

RESULTS

Expression of *miR-30b* and *30d* in Human Melanoma Marks the Progression from Primary to Metastatic Tumors

miRNA array analysis of 59 metastatic melanoma tumor samples (Segura et al., 2010), followed by quantitative RT-PCR (qRT-PCR) validation, revealed relatively high expression levels of *miR-30b* and *-30d*. These two miRNAs form a cluster on 8q24, a common amplicon in melanoma (Ehlers et al., 2005). No statistically significant upregulation of *miR-30b/30d* was observed from congenital nevi to primary melanomas (see Figure S1A available online). However, in a subset of 17 paired samples (primary tumor and a metastasis from the same patient), we found a statistically significant increase in expression of these miRNAs from the primary to the metastatic stage (p = 0.0007 for *miR-30b*; p = 0.026 for *miR-30d*) (Figure 1A). A miRNA profile of primary melanomas (n = 92; Table S1) revealed that

higher levels of *miR-30b* and *-30d* correlated with increased tumor thickness (p = 0.002 for *miR-30b*, p = 0.0002 for *30d*) (Figure 1B) and advancing stage (I–III) (p = 0.004 for *miR-30b*, p = 0.001 for *30d*; Figure 1C), suggesting an association between *miR-30b*/d expression and tumor progression. By histological subtype the more invasive nodular melanomas had higher *miR-30b/30d* levels than superficial spreading melanomas (SSMs) (p = 0.015 for *miR-30b*, p = 0.0189 for *30d*) (Figure 1D). Furthermore, the subgroup of primary melanomas that had metastasized (n = 44) showed higher levels of *miR-30b* and *-30d* expression than those that had not spread (n = 48) during a period of 24 months or more of follow-up (p = 0.048 for *miR-30b*, p = 0.037 for *miR-30d*; data not shown). Accordingly, *miR-30b* and *miR-30d* levels above the median correlated with shorter time to recurrence (p = 0.04 for *miR-30b* and p = 0.01 for *miR-30d*) (Figure 1E) and lower overall survival of patients with melanoma (p = 0.0004 for *miR-30b* and p = 0.02 for *miR-30d*) (Figure 1F). Multivariate analysis using COX PH models indicated that the expression level of *miR-30d* is a statistically significant independent predictor for melanoma mortality (p = 0.004) when adjusted for primary tumor thickness and ulceration status. The expression level of *miR-30b* is only marginally significant as an independent predictor for death with melanoma when adjusted for primary tumor thickness and ulceration (p = 0.054). These data support an association between *miR-30b/30d* upregulation and increased melanoma aggressiveness, and suggest a potential use of these miRNAs as prognostic biomarkers.

miR-30b/30d Overexpression Correlates with Genomic Amplification in a Subset of Human Melanoma Samples

The *miR-30b/30d* cluster (8q24.22–8q24.23) is located in the vicinity of a genomic region containing the oncogene *c-MYC* (8q24.21), which is frequently amplified in multiple cancer types, including: medulloblastoma (Lu et al., 2009); uveal melanoma (Ehlers et al., 2005); head, neck, and cervical squamous cell carcinomas; and bladder (Visapää et al., 2003), lung, and prostate cancer (Van Den Berg et al., 1995). *c-MYC* amplification is usually associated with tumor progression.

We found the *miR-30b/30d* genomic region amplified in 12 out of 33 metastatic melanoma tissues (36.4% of cases, Figure S1B), of which approximately half harbored concomitant *c-MYC* gene copy gains (Figure S1C), suggesting that the *miR-30b/30d* gains are generally independent of *c-MYC* amplification. Interestingly, we noted that a higher fraction of patients carrying the *miR-30b/30d* amplification died within the study period (Figure S1B), suggesting that this genetic trait is associated with more aggressive disease.

miR-30b or *miR-30d* Modulation Alters the Invasive Potential of Melanoma Cells without Affecting Cell Proliferation

Because upregulation of *miR-30b* and *30d* is associated with progression from primary to metastatic melanoma, we asked whether these miRNAs enhance the invasive behavior of melanoma cells. Using a fibronectin transwell invasion assay, we found that ectopic expression of *miR-30b* and *30d* (Figure S2A) strongly stimulated the invasive capacity of two metastatic melanoma cell lines, 113/6-4L (hereafter, 4L) and 131/4-5B1 (hereafter 5B1) (Cruz-Munoz et al., 2008) (Figure 2A) (p = 0.037 and p = 0.0002 for *miR-30b* and p = 0.009 and p = 0.011 for *miR-30d* in 4L and 5B1, respectively). In contrast, silencing of *miR-30b* or *miR-30d* by antisense oligonucleotide (anti-miR) transfection (Figure S2A) suppressed cell migration (p = 0.026 and p = 0.032 for *miR-30b*; p = 0.041 and p = 0.044 for *miR-30d* in 4L and 5B1, respectively) (Figure 2A).

To determine whether the increase in invasive behavior could be explained, at least in part, by increased cell proliferation, we compared the growth rates of cells transduced with *miR-30b* or *miR-30d* or scrambled control. We found no statistically significant differences by means of trypan blue exclusion or crystal violet staining (data not shown). Therefore, we conclude that *miR-30b/30d* increase melanoma cells' capacity to migrate through the extracellular matrix, an essential ability for metastasis.

Next, because *miR-30b* and *miR-30d* are coexpressed from the same cluster, we tested the effect of introducing both simultaneously. Neither additive nor synergistic effects were detected in the Boyden chamber assay (Figure 2A), indicating that the two miRNAs have redundant proinvasive functions. This is not surprising because they share the same seed region and, thus, likely operate through common targets.

miR-30b/30d Overexpression Enhances Metastasis, Whereas *miR-30d*'s Silencing Represses Metastasis In Vivo

Our in vitro results led us to study the impact of *miR-30d* downregulation in a classic in vivo model of lung metastasis: we transiently transduced B16F10 mouse melanoma cells in vitro with scrambled or anti-*miR-30d* oligonucleotides (Figure S2B) and injected them into the tail veins of immunocompetent mice 8–weeks of age. Eleven days postinjection, we sacrificed the mice and dissected the lungs for macroscopic and microscopic histology. Lungs of B16F10/anti-*miR-30d*-injected mice harbored significantly fewer microscopic and macroscopic metastases than scrambled control (p = 0.0085) (Figure 2B). Conversely, mice injected with B16F10 cells transiently transduced with *miR-30d* mimic oligonucleotides generated more metastatic foci than control cells transfected with scrambled oligonucleotide (p = 0.0218) (Figure 2C). Then, we compared the metastatic potential of B16 transiently transfected with *miR-30b*, *miR-30d*, or combinations of *miR-30b* and *30d* mimic oligonucleotides, injected through the tail vein. *miR-30d* and *miR-30b* had similar prometastatic effects, and the combination of the two showed only a slight increase over *miR-30d* alone (Figures S3A–S3C). Therefore, both our in vitro and in vivo results indicate that *miR-30b* and *miR-30d* have redundant effects on invasion and metastasis. Given this functional redundancy, we focused primarily on *miR-30d* in the following experiments.

We asked whether *miR-30d* could confer metastatic potential to melanoma cells significantly less invasive, such as the primary melanoma cells WM35 and WM98. In vitro invasion assays revealed that ectopic expression of *miR-30d* dramatically enhanced the invasive capacity of WM35 and WM98 primary human melanoma cells (p < 0.001 for both cell lines) (Figure 2D). In vivo, WM98 cells display very poor seeding and colonization of mouse lungs upon tail vein injection, but *miR-30d* upregulation

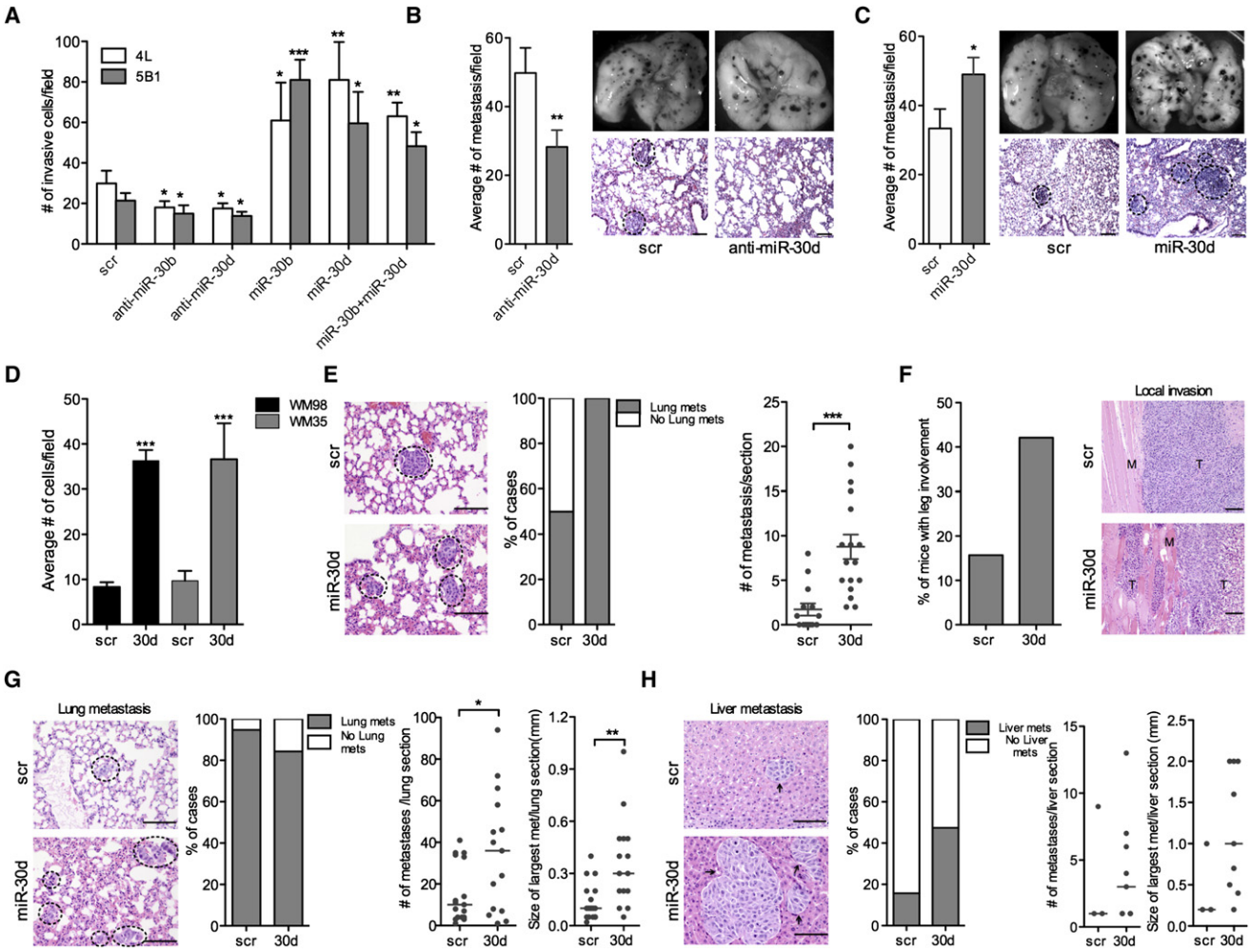

Figure 2. *miR-30b* and *miR-30d* Promote Melanoma Invasion and Metastasis In Vitro and In Vivo

(A) Transwell invasion assay of indicated cell lines with *miR-30b*, *-30d*, or both, either silenced or overexpressed (mean ± SEM). scr, scrambled control.

(B and C) In vivo metastasis assay with B16F10 mouse melanoma cells transfected with scr, anti-*miR-30d*, or *miR-30d* mimics injected through the lateral tail vein of C57BL/6J mice. Histogram in (B) shows that anti-*miR-30d* suppressed metastasis, whereas *miR-30d* increased the metastatic behavior (C) (mean ± SEM). On the right are macroscopic pictures of mouse lungs and H&E sections of lung metastases at termination of the experiment. Black dotted circles mark metastatic foci.

(D) Transwell invasion assay with primary melanoma cell lines WM98 and WM35 transduced with scr or *miR-30d* (mean ± SEM).

(E) In vivo metastasis assay with WM98 melanoma cells stably transduced with GIPZ-scr or GIPZ-*miR-30d* injected through the lateral tail vein of NOG/SCID mice. Histogram shows the percentage of mice that developed lung metastases in each cohort. Whisker plots show the distribution of the number of metastases per section. Representative H&E sections of lungs are shown. Black dotted circles mark metastatic foci.

(F–H) Preclinical model of human melanoma metastasis. 5B1 cells stably transduced with either scr or *miR-30d* vectors were injected subcutaneously into the flanks of NOG/SCID mice.

(F) H&E sections show increased local invasion of *miR-30d*-transduced tumors. Histogram represents the percentage of mice in each cohort with primary tumors that invaded grossly into the leg. M, muscle; T, tumor.

(G and H) Representative micrographs of H&E sections of lungs (G) or livers (H) are presented. Histograms depict the percentage of mice that developed lung or liver metastases in each cohort. Whisker plots show the distribution of the number or size (largest in each section) of metastasis per section. Error bars represent the median value (*$p < 0.05$; **$p < 0.01$; ***$p < 0.001$). For all micrographs scale bars represent 100 μm.

See also Figure S2.

dramatically increased both the incidence of lung metastasis and the total number of micrometastasis per lung section (Figure 2E). These in vitro and in vivo results evidence the strong prometastatic potential of this miRNA.

Given the limitations of the tail vein injection models at recapitulating all the steps of metastasis, we decided to test the effects of *miR-30d* in a more preclinical system, in which human melanoma cells are injected in the flanks of immunocompromised mice. These mice form a tumor mass within about 2 weeks, from which cells migrate and reach the lungs in 8–10 weeks with occasional spread to the liver and other organs (Cruz-Munoz et al., 2008). 5B1 cells stably transduced with lentiviruses carrying pre-*miR-30d* (GIPZ/*miR-30d*) or a scrambled sequence (GIPZ/scr) were inoculated in the flanks

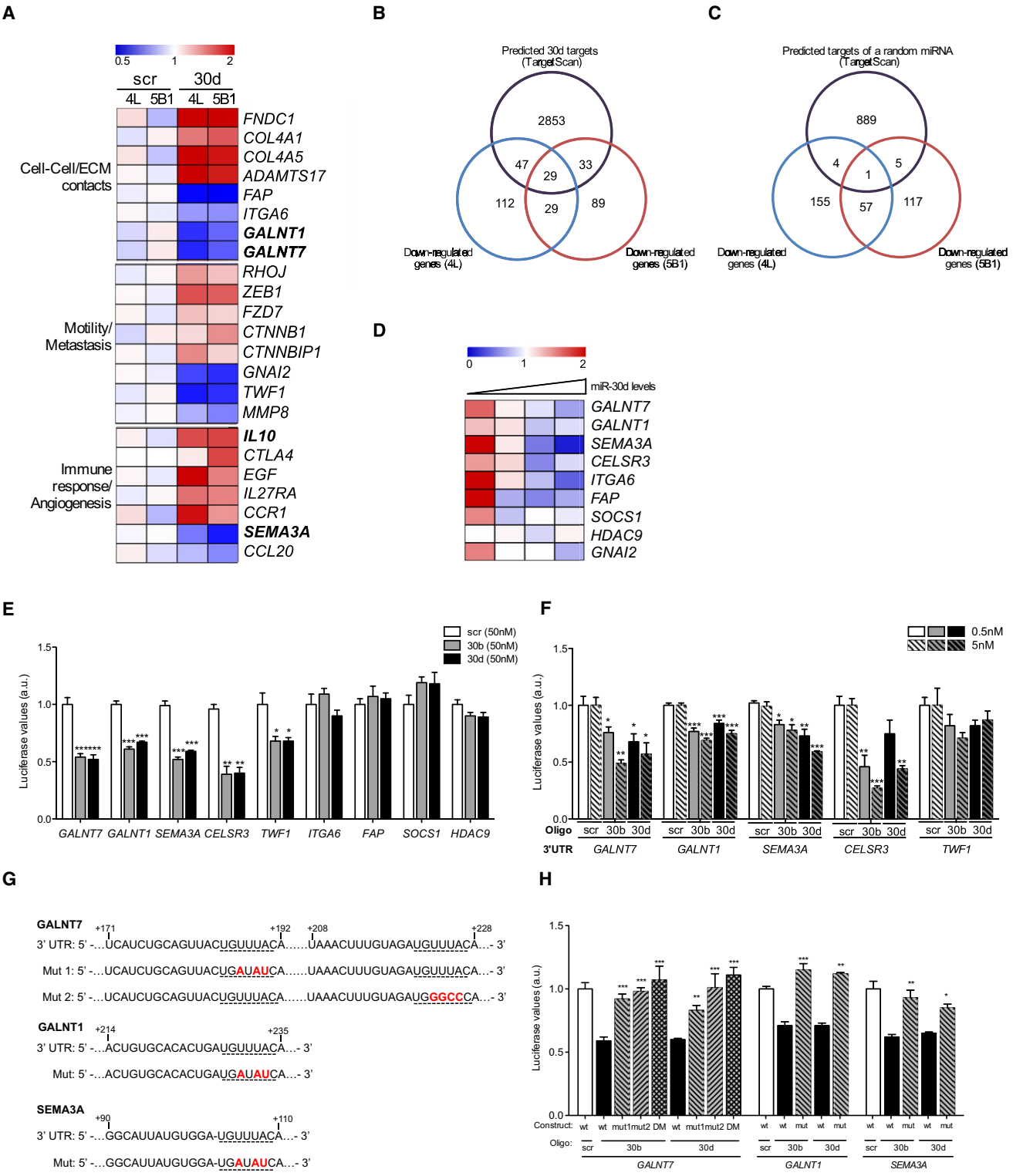

Figure 3. *miR-30b/30d* Directly Target SEMA3A, TWF1, CESLR3, GALNT7, and GALNT1

(A–C) Microarray analysis performed in independent biological duplicates for each indicated cell line.

(A) Heat map showing the average normalized relative expression levels of genes involved in cell-cell/ECM contacts, motility, metastasis, immune response, or angiogenesis in the indicated cell lines transfected with either scr or *miR-30d* mimics.

(B) Venn diagram depicting the overlap between predicted *miR-30d* targets (TargetScan) and probes significantly downregulated in response to *miR-30d* overexpression in two cell lines.

of NOD/Shi-*scid*/IL-2Rγ^{nul} (NOG/SCID) mice. Local muscle invasion involving the proximal leg was more commonly found among the GIPZ/*miR-30d*-injected mice than in the GIPZ/scr group (Figure 2F). Moreover, the proportion of mice that developed liver metastases at completion of the experiment was higher in the *miR-30d* cohort (9 of 19) than in the scramble cohort (3 of 19) (Figure 2H) ($p = 0.038$). Both the number and size of lung and liver micrometastases found 11 weeks after the initial injection were elevated in mice of the GIPZ/*miR-30d* cohort (Figures 2G and 2H). These data demonstrate that *miR-30d* augments the ability of melanoma cells to intravasate, extravasate, seed, and/or colonize a distant site.

GALNT7, GALNT1, SEMA3, CELSR3, and TWF1 Are *miR-30b/30d* Targets in Melanoma Cells

To identify cellular pathways modulated by *miR-30d* upregulation and to define specific gene targets that might mediate its prometastatic effects, we conducted a global transcriptome analysis of 4L and 5B1 cells transduced with *miR-30d* or scrambled oligonucleotides using Affymetrix arrays. Using thresholds of a minimum fold change of 1.33 and a p value of <0.05, we found 784 genes to be differentially expressed by the 2 cell lines. Gene ontology analysis revealed candidate genes whose altered expression could contribute to the invasive phenotype induced by *miR-30d* (Figure 3A). Of the 784 altered genes, we found 217 genes downregulated in 4L, 180 downregulated in 5B1, and 58 downregulated in both lines. Nearly one-third of the downregulated genes were direct *miR-30d* targets predicted by public algorithms (TargetScan) (Lewis et al., 2005) (Figure 3B), and included *GNAI2*, a validated *miR-30d* target (Yao et al., 2010). Meanwhile, the overlap with targets of a randomly selected miRNA was minimal (Figure 3C). Interestingly, data mining of our previously published mRNA profile of human metastatic melanoma tissues (Bogunovic et al., 2009) revealed that *miR-30d* levels inversely correlate with expression of several targets identified in our array analysis, including SEM*A3A*, *GALNT1*, and *GALNT7* (Figure 3D), further supporting the physiological relevance of this regulatory mechanism. The expression levels of other *GALNT* family members, many of which carry recognition sites for *miR-30d* in their 3′ untranslated regions (UTRs), also inversely correlated with *miR-30d* levels in those tissues (Figure S4). Using 3′UTR luciferase reporter assays and qRT-PCR, we confirmed that *GALNT7*, *GALNT1*, *SEMA3*, *CESLR3*, and *TWF1* are direct targets of *miR-30b/30d* (Figures 3E and 3F). Mutations in the miRNA recognition sites (Figure 3G) rendered the constructs unresponsive to *miR-30b* or *miR-30d* induction (Figure 3H), further confirming that these are direct *miR-30b/30d* targets.

GALNT7 Is a Critical Mediator of *miR-30d* Proinvasive Effects In Vitro and Prometastatic Behavior In Vivo

Next, we investigated which, if any, *miR-30d* direct targets mediate the capacity for cellular invasion. Several candidates seemed appealing: CELSR3 is involved in contact-mediated cell-to-cell communication (Wu and Maniatis, 1999); TWF1 encodes for twinfilin (Palmgren et al., 2002), which regulates cell motility; and Semaphorin 3A (SEMA3A) exerts antiangiogenic properties (Maione et al., 2009). GalNAc transferases (GalNAc-Ts) initiate mucin-type O-linked glycosylation in the Golgi apparatus by catalyzing the transfer of N-acetylgalactosamine (GalNAc) to serine and threonine residues on target proteins. These posttranslational modifications affect the structure of numerous transmembranal substrates, determining their functional interaction with the extracellular environment (Ten Hagen et al., 2003).

Given their described roles, all these molecules seemed plausible candidates to shape the prometastatic influence of *miR-30b/30d*. To determine whether any of them were critical mediators of *miR-30d*'s role in cellular invasion, we silenced each of them using RNA interference (RNAi) in melanoma cell lines. Although downregulating SEM*A3A*, *CELSR3*, and *TWF1* did not enhance invasion, repression of *GALNT7*, and to a lesser extent *GALNT1*, recapitulated the proinvasive effects of *miR-30d* ($p < 0.0001$ for *GALNT7*; $p = 0.004$ for 5B1 and 0.01 for A375 for *GALNT1*) (Figure 4A; Figure S2C). Moreover, coexpression of a *GALNT7* cDNA lacking the 3′UTR was able to suppress *miR-30d* promotion of cell invasion, indicating that GALNT7 silencing critically mediates *miR-30d*'s promigratory effects in melanoma ($p < 0.0001$) (Figure 4B; Figure S2D).

GALNT7 silencing by siRNA oligonucleotides was able to mirror *miR-30d*'s promotion of B16F10 metastatic capacity upon tail vein injection ($p = 0.0006$) (Figure 4C). Finally, we compared the metastatic potential of B16F10 cells transduced with *miR-30d* oligonucleotides and either an empty lentiviral vector or one expressing the murine GALNT7 cDNA. Concomitant ectopic expression of GALNT7 and *miR-30d* interfered with *miR-30d*'s prometastatic effect ($p = 0.0002$) (Figure 4D). Overall, our in vitro and in vivo data support GALNT7 inhibition as a key contributor of *miR-30d*'s prometastatic effects in melanoma cells.

miR-30d Overexpression and GALNT7 Inhibition Produce Similar Glycomic Changes, which Are Rescued by GALNT7 Ectopic Expression

We hypothesized that inhibiting GALNT7 could promote cell invasion by modifying the O-glycosylation patterns of membrane proteins that interact with the extracellular matrix and cells of the

(C) Venn diagram illustrating the overlap between predicted targets of an unrelated miRNA (*miR-199a-3p*) and genes significantly downregulated in response to *miR-30d* overexpression in two cell lines.

(D) Heat map depicting the expression levels of selected predicted targets in 18 human metastatic melanoma tissues with increasing levels of *miR-30d*. Each column represents an average expression of four to eight samples with similar *miR-30d* levels. See also Figure S4.

(E) Reporter assay in 293T cells transfected with *miR-30b* or *miR-30d* and constructs carrying the luciferase cDNA fused to the 3′UTR of selected predicted targets (mean ± SEM).

(F) Reporter assay in 293T cells transfected with luciferase constructs fused to the 3′UTR of *GALNT7*, *GALNT1*, *SEMA3A*, *CESLR3*, and *TWF1* and significantly lower concentrations of *miR-30b/30d* (mean ± SEM).

(G and H) Reporter assay in 293T cells transfected with luciferase constructs carrying *GALNT7*, *GALNT1*, and *SEMA3A* 3′UTRs mutated in *miR-30b/30d*-binding sites. DM, double mutant (mean ± SEM). (*$p < 0.05$; **$p < 0.01$; ***$p < 0.001$).

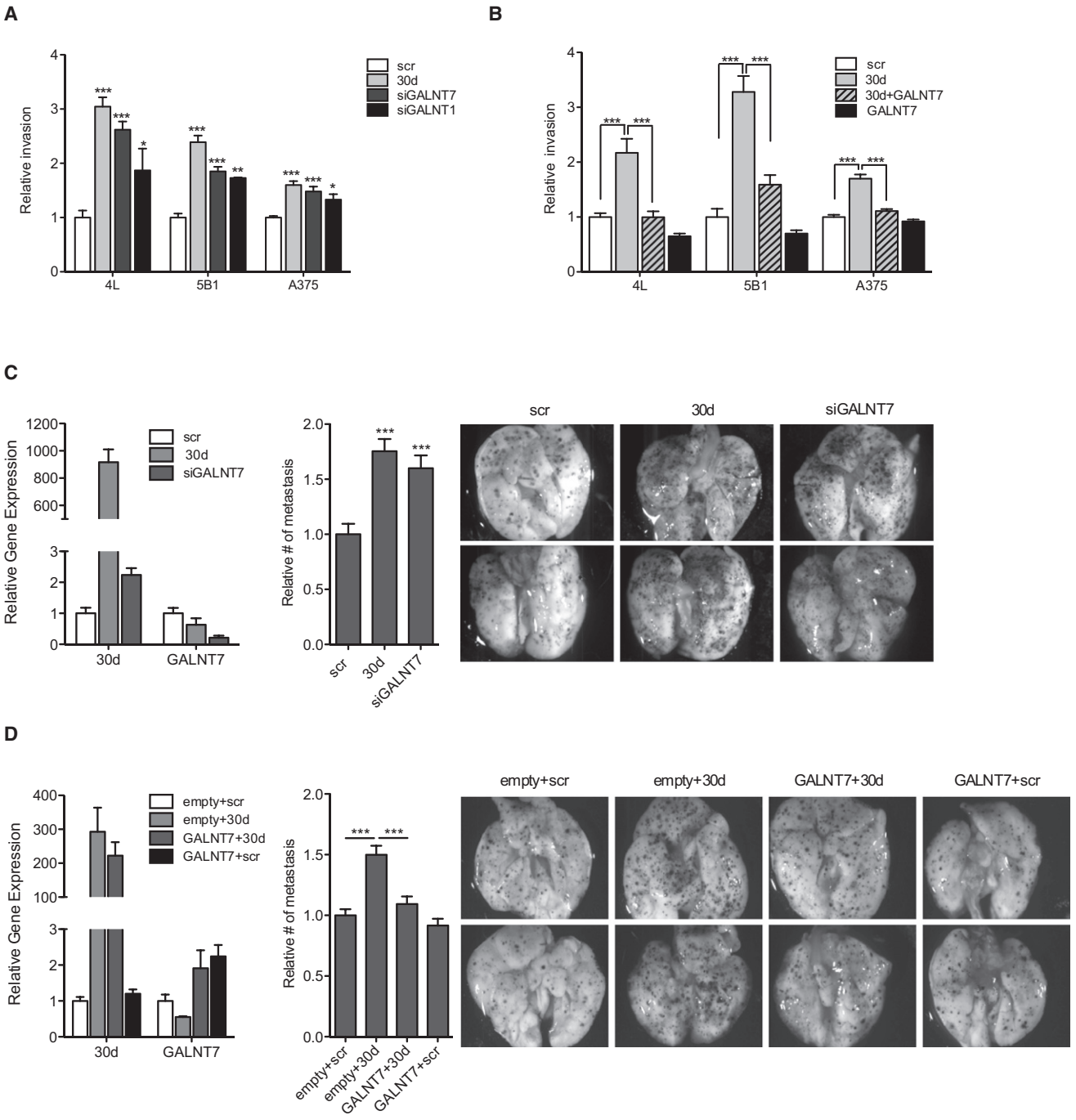

Figure 4. GALNT7 Modulation Accounts for *miR-30d* Proinvasive Effects In Vitro and In Vivo

(A and B) Transwell invasion assay of indicated cell lines transfected with scr, *miR-30d*, si*GALNT7*, si*GALNT1*, *GALNT7* cDNA, or cotransfected with *miR-30d* and *GALNT7* cDNA (mean ± SEM).

(C and D) In vivo metastasis assay with B16F10 mouse melanoma cells.

(C) Cells were transfected with scr, *miR-30d* mimics, or siGALNT7 oligos and injected through the lateral tail vein of C57BL/6J mice. Levels of knockdown or overexpression are shown on the left. Histogram and macroscopic pictures are shown.

(D) Cells were stably transduced with either pEIGW-Empty or pEIGW-mmuGALNT7. Twenty-four hours prior to injection, cells were transfected with either scr control or *miR-30d* oligonucleotides. Cells were injected through the lateral tail vein of NOG/SCID mice. Levels of overexpression are shown on the left. Histogram and representative macroscopic pictures are depicted (mean ± SEM; *p < 0.05; **p < 0.01; ***p < 0.001).

See also Figure S3.

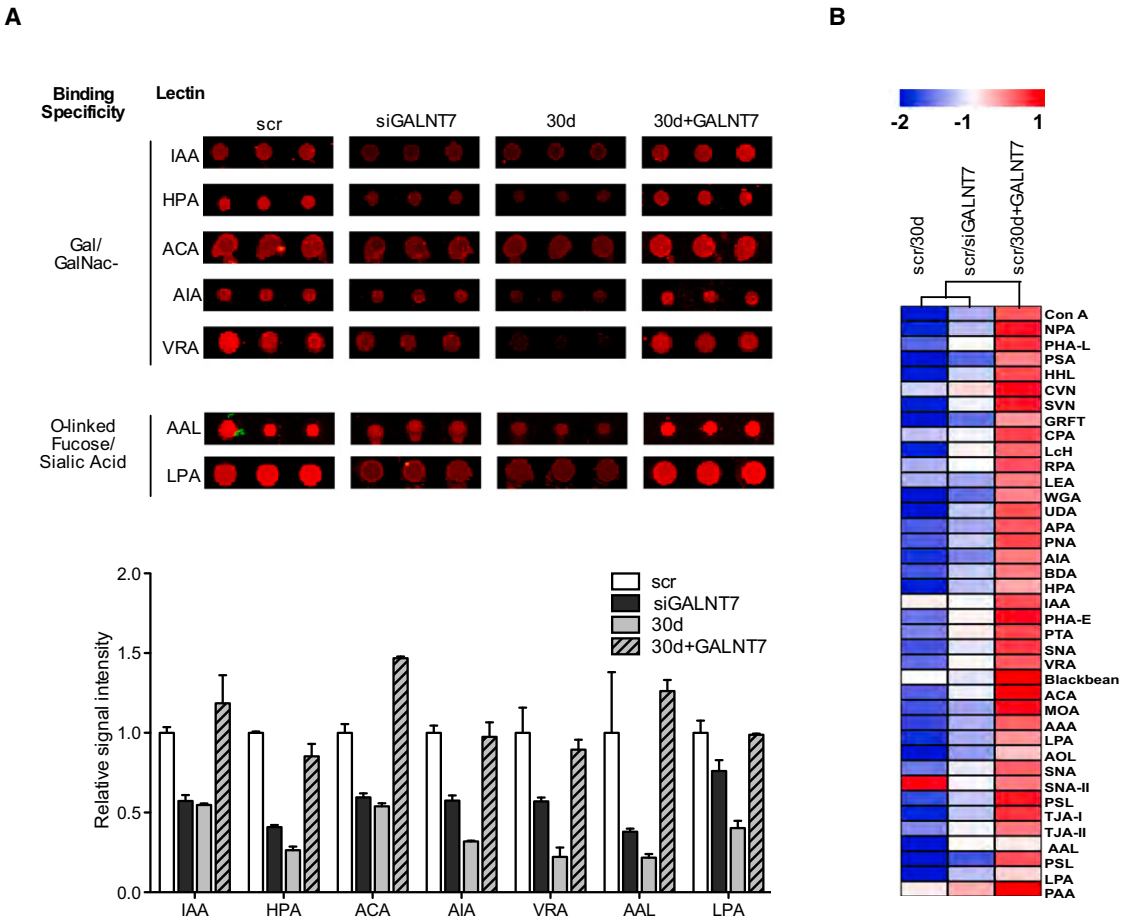

Figure 5. GALNT7 Modulation Accounts for *miR-30d*-Mediated Alterations in Membranous O-Linked Glycans

Lectin microarray analysis of 5B1 cells transiently transfected with scrambled control, *miR-30d*, si*GALNT7*, or cotransfected with both *miR-30d* and *GALNT7* cDNA. (A) Array spots (in triplicates) showing raw signal intensities of galactosamine- or N-Acetylgalactosamine (Gal/GalNAc)-, fucose-, or sialic acid-binding lectins in the four treatment groups. The similarities and differences are quantitated in the histogram that represents the average relative binding signal intensity of the lectins depicted above (mean ± SEM). (B) Heat map representing normalized signal intensity of a dual-color lectin array. Each treatment sample (labeled with Cy3) was hybridized in a 1:1 molar ratio with a scr sample (labeled with Cy5) as internal control. See also Figure S5.

tumor microenvironment. To test this hypothesis, we obtained glycomic profiles of melanoma cells transfected with *miR-30d* only, *siGALNT7* only, *miR-30d* together with *GALNT7* cDNA, and scrambled-control miRNA, using lectin microarrays consisting of 84 discrete carbohydrate-binding proteins (Krishnamoorthy et al., 2009). We analyzed cellular micellae from isolated cell membranes, which previous work has shown to contain both glycoproteins and glycolipids representative of the cell surface (Pilobello et al., 2005). Our lectin microarray analysis revealed an overall decrease in glycosylation in both siGALNT7 and miR*30d*-transduced cells relative to scrambled control, affecting both N- and O-linked glycosylation (Figure S5). The most pronounced conserved effects across both *miR-30d* and siGALNT7, based on single color array data, were on secondary modifications such as fucose and sialic acid as well as terminal GalNAc, confirming a predominant effect on O-linked glycosylation (Figure 5A). Importantly, cotransfection of GALNT7 cDNA rescued these glycosylation defects for both N- and O-linked glycans (Figure 5A; Figure S5A). To facilitate direct comparisons among samples, we utilized a more sensitive ratiometric two-color approach (Krishnamoorthy et al., 2009) in which cell membrane micellae from scrambled-transduced cells served as a common biological reference. These data confirmed the observed general reduction in both N- and O-linked glycosylation (Figure 5B; Figure S5B). Similar but not completely overlapping changes were induced by siGALNT1 (data not shown). That similar glycosylation changes are induced by both *miR-30d* upregulation and *siGALNT7*, and are restored by reexpressing GALNT7, support the key contribution of GALNT7 repression to *miR-30d*-associated phenotypes. It is likely that those modified glycosylation patterns act as direct or indirect mediators of *miR-30d*'s prometastatic role.

In order to determine the contribution of chemokine receptor signaling to the prometastatic role of *miR-30d*, we investigated the effects of blocking intracellular signaling by incubating the melanoma cells with Pertussis toxin (PTX), which is known to catalyze the ADP-ribosylation of the α subunits of the heterotrimeric G protein, and prevents Gi proteins from interacting with G protein-coupled receptors on the cell membrane.

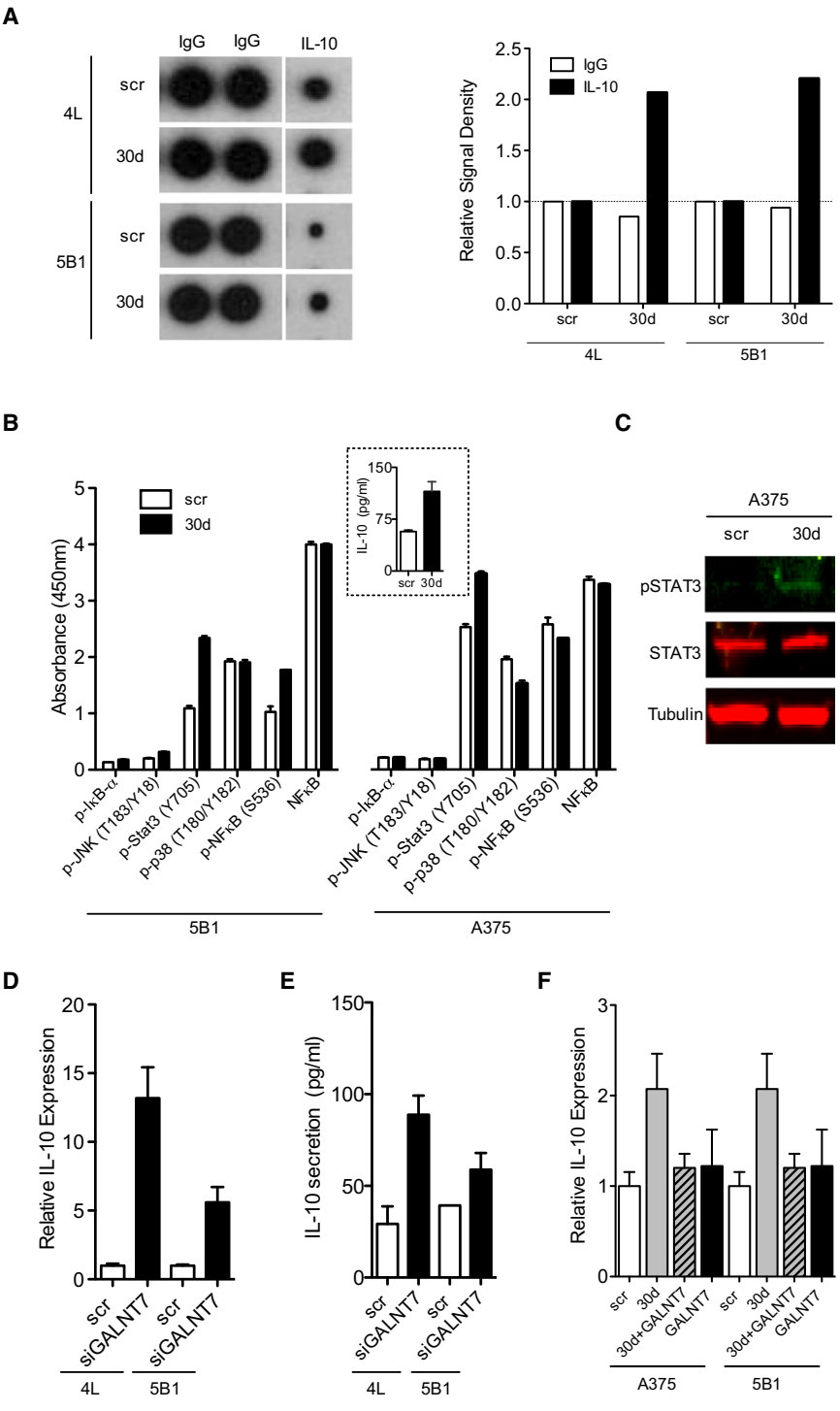

Figure 6. *miR-30d* Promotes IL-10 Secretion by Suppressing GALNT7

(A) Levels of IL-10 in melanoma cells transduced with *miR-30d* relative to scr control measured by cytokine array. Quantification of signal density is presented on the right.

(B) Levels of phosphorylation of proteins that might explain the increase in IL-10 secretion from *miR-30d*-transfected cells as measured by solid-phase ELISA in indicated cell lines. Inset shows levels of IL-10 secreted from the cells, quantified by ELISA (mean ± SEM).

(C) Western blot of phospho-STAT3 levels in scr or *miR-30d*-transfected cells. Tubulin served as loading control.

(D) IL-10 mRNA levels in siGALNT7-transfected melanoma cell lines 4L and 5B1 relative to scr control as measured by qRT-PCR (mean ± SEM).

(E) Secretion of IL-10 to the supernatant of siGALNT7-transfected or scr-transfected melanoma cell lines, as measured by ELISA.

(F) IL-10 mRNA (measured by qRT-PCR) levels in indicated melanoma cells transfected with scr, *GALNT7* cDNA, or cotransfected with both *miR-30d* and GALNT7 (mean ± SEM).

See also Figure S6.

Pretreatment of melanoma cells with PTX (100 ng/ml; 24 hr) had little to no effect on *miR-30d*'s prometastatic potential in a tail vein injection experiment (Figure S6). This suggests that Gi-dependent chemokine signaling does not contribute significantly to the effects of *miR-30d* or GALNT7 on extravasation, seeding, or colonization, but we cannot rule out a Gi-independent chemokine signaling.

miR-30d Stimulates the Expression of the Immunosuppressive Cytokine Interleukin-10 by Repressing GALNT7

Our microarray analyses in two independent cell lines revealed that *miR-30d* ectopic expression results in mRNA upregulation of some immune modulators, among them the immunosuppressive immunoglobulin CTLA4 and the immunosuppressive cytokine IL-10 (Figure 3A). Using human cytokine antibody arrays and ELISA, we confirmed that melanoma cells transfected with *miR-30d* and *30b* mimics secrete significantly more IL-10 than scrambled controls (Figures 6A and 6B; Figure S3D). In search of a mechanism accounting for *miR-30d*-mediated induction of IL-10, we tested the effect of *miR-30d* on the major signaling pathways known to modulate IL-10 levels (i.e., PI3K, STAT3, NF-κB, p38MAPK, JNK). Melanoma cells that overexpress *miR-30d* displayed increased levels of phospho-Tyr705-STAT3 (Figures 6B and 6C), which is known to transcriptionally activate IL-10 as well as numerous prometastatic genes (Yu et al., 2009). Although STAT3 activation could partially explain the elevated IL-10 expression, we asked whether any of our identified *miR-30d* direct targets could contribute to it. Surprisingly, we found that GALNT7 silencing is sufficient to induce IL-10 synthesis and secretion to levels comparable to those induced by *miR-30d* (Figures 6D and 6E)

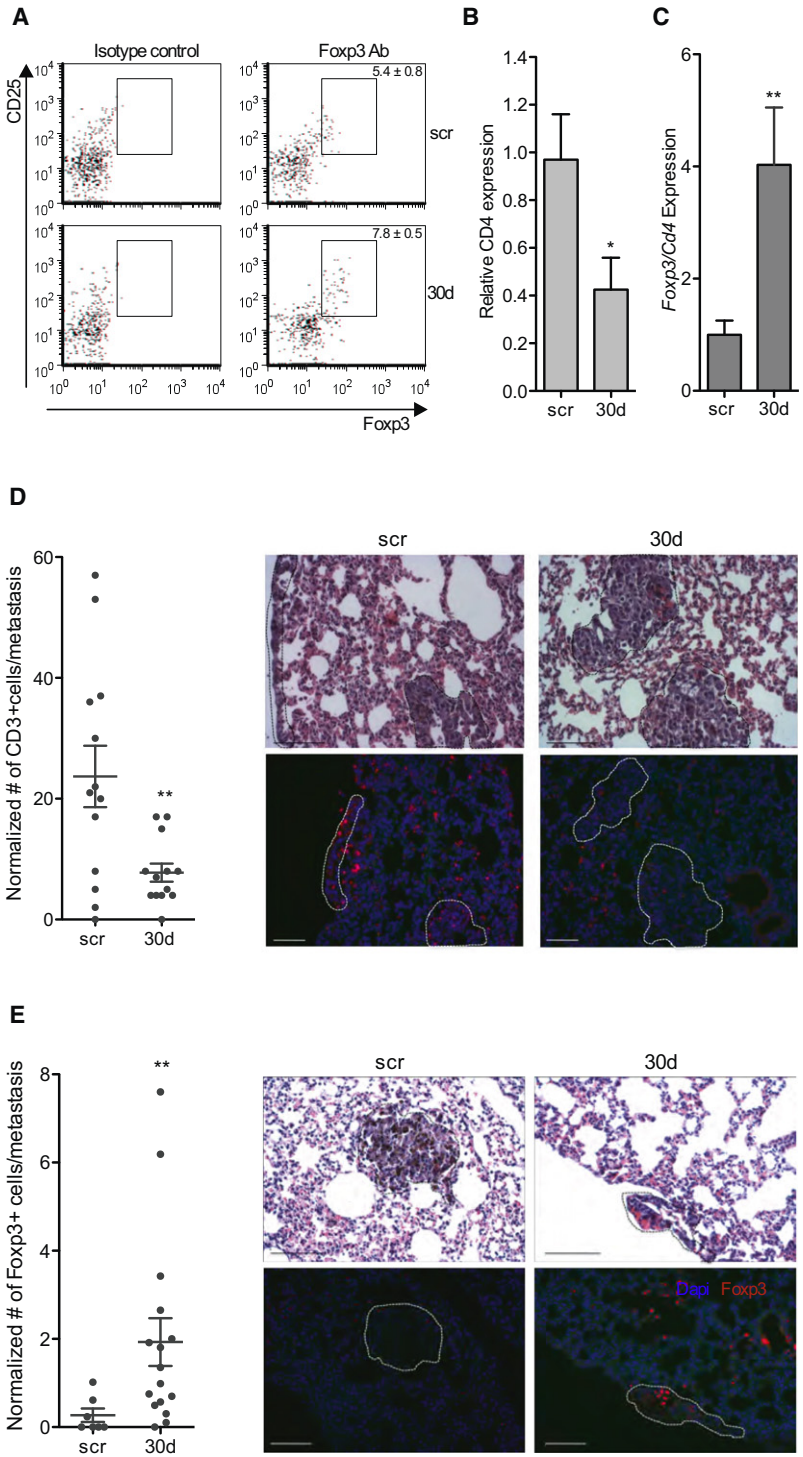

Figure 7. *miR-30d* Associates with Enhanced Immunosuppressive Features at the Metastatic Site

(A) Representative flow cytometry of Tregs ($CD4^+$ $CD25^+$ $Foxp3^+$) isolated from whole lungs of mice injected with B16F10/scr or B16F10/*miR-30d* (mean ± SEM). Isotype controls are shown on the left for each treatment group. See also Table S2.

(B) CD4 mRNA levels in macrometastases dissected from B16F10/*miR-30d* relative to B16F10/scr-injected mice (mean ± SEM).

(C) Foxp3 mRNA expression in macrodissected metastases extracted from lungs of mice injected with B16F10/*miR-30d* relative to B16F10/scr cells (mean ± SEM).

(D) CD3 immunofluorescence staining shows recruitment of T cells to metastases of either B16F10/*miR-30d* or B16F10/scr-injected mice. Corresponding H&E on consecutive sections are shown in upper panels, and metastatic foci are circled. Scatter plot depicts the number of recruited CD3+ T cells to the metastasis in several mice per group. The number of recruited cells was normalized to the area of metastasis.

(E) FoxP3 immunofluorescence staining shows recruitment of regulatory T lymphocytes to B16F10/*miR-30d* compared to B16F10/scr metastases. Corresponding H&E on consecutive sections are shown in upper panels, and metastatic foci are circled. Scatter plot depicts the number of recruited CD3+ T cells to the metastasis in several different mice for each group. Scale bars represent 100 μm (*$p < 0.05$; **$p < 0.01$).

See also Figure S7.

or *miR-30b* (Figure S3D), and that GALNT7 overexpression counteracts *miR-30d* (Figure 6F) or *miR-30b*-mediated (Figure S3D) IL-10 upregulation. These results suggest that *miR-30d/30b* induce IL-10 at least in part by repressing GALNT7, revealing an unexpected role for a single GalNAc-T in linking tumor cell invasion and immune modulation.

miR-30d Upregulation Triggers Immunosuppressive Properties at the Metastatic Site

To determine whether aberrant *miR-30d* expression is able to promote an immunosuppressive environment in vivo, we compared the recruitment of T cells (CD3+), regulatory T cells (Tregs; $CD4^+CD25^+Foxp3^+$), activated dendritic cells (DCs; $MHCII^+F480^-CD86^+$), and myeloid-derived suppressor cells (MDSCs; $CD11b^+Gr1^+$) to the lungs of immunocompetent mice injected with B16F10/scr or B16F10/*miR-30d* cells through the tail vein. FACS analysis showed that lungs of B16F10/*miR-30d*-injected mice contain significantly more Tregs ($p = 0.03$) (Figure 7A) than the equivalent scrambled controls, with moderate changes in activated DCs and no significant changes in MDSCs (Table S2). Differences were more prominent when individually macrodissected metastases were analyzed; we noted that metastases from mice injected with B16F10/*miR-30d* displayed lower local levels of CD4 mRNA ($p = 0.039$) (Figure 7B) and higher levels of *Foxp3* mRNA (normalized to CD4 levels in the tissue; $p < 0.01$) (Figure 7C) than those from mice injected with B16F10/scr cells. Immunofluorescence stainings confirmed both the reduction in T cell accrual (Figure 7D) and the increased recruitment of Tregs to the metastases of B16F10/*miR-30d* cells (Figure 7E). In accordance, immunohistochemistry analysis of

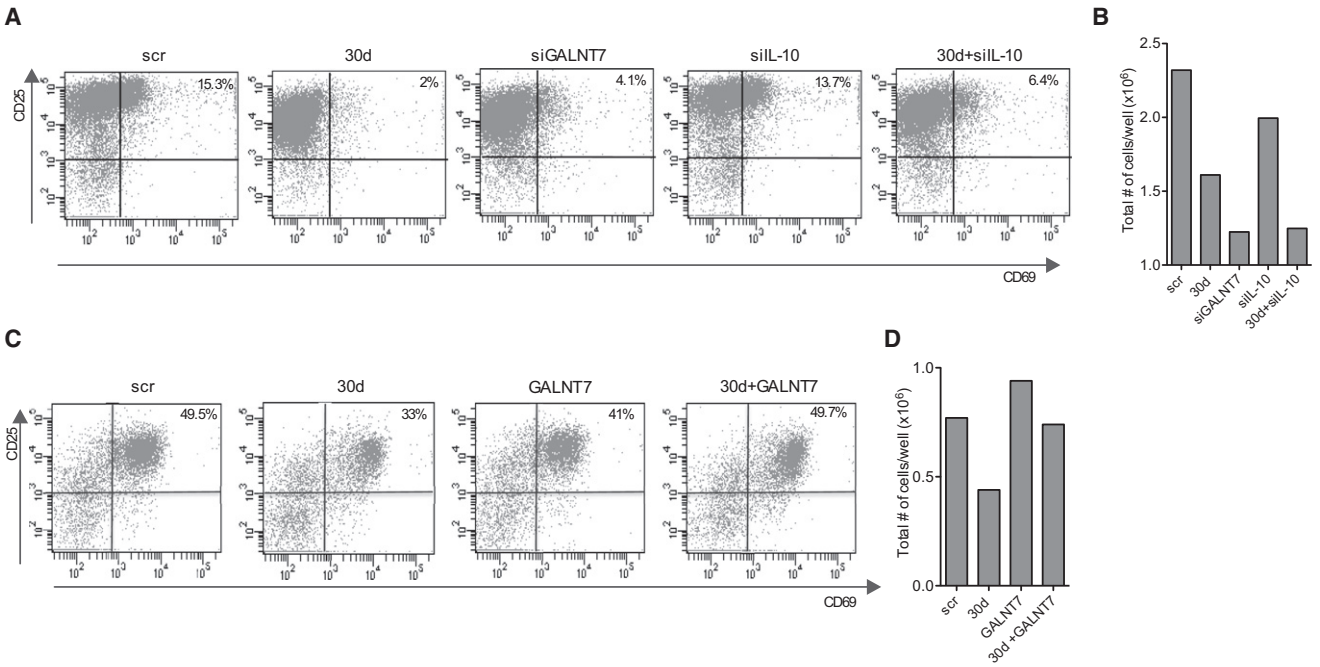

Figure 8. GALNT7 Modulation Accounts for *miR-30d*-Mediated Immunosuppressive Effects Ex Vivo

(A) FACS analysis of activated (CD25+CD69+ gated on CD4+) T lymphocytes isolated from spleens of *Foxp3*-GFP mice, stimulated by CD28 and CD3 antibodies, and incubated for 72 hr in the presence of supernatants from A375 melanoma cells transfected with scr, *miR-30d*, siGALNT7, siIL10, and *miR-30d*+siIL-10.

(B) Total number of T cells at conclusion of the experiment (representative experiment, n = 3).

(C) FACS analysis of activated (CD25+CD69+ CD4+) T lymphocytes isolated from spleens of *Foxp3*-GFP mice, stimulated by CD28 and CD3 antibodies, and incubated for 72 hr in the presence of supernatants from 5B1 melanoma cells transfected with scr+pCDNA3-Empty (scr), *miR-30d*+pCDNA3-Empty (30d), scr+pCMV-GALNT7 (GALNT7), and *miR-30d*+pCMV-GALNT7 (30d+GALNT7).

(D) Total number of T cells at conclusion of the experiment (a representative experiment).

human metastatic melanomas (n = 32) revealed some association between *miR-30d* levels and FOXP3 expression in infiltrating lymphocytes (p = 0.11; data not shown). Interestingly, we found a significant correlation between FOXP3 expression and *miR-30d* levels in the tumor cells themselves (n = 45; p = 0.02) (Figure S7A). To confirm that FOXP3 is indeed expressed by melanoma cells, we conducted HMBA-45 immunohistochemistry stainings in consecutive tissue sections (Figure S7B). Overall, these results suggest that *miR-30d* might contribute to metastasis not only by promoting migration but also by suppressing immune surveillance.

In order to explore the mechanism of immune modulation by *miR-30d*, we tested the ability of *miR-30d* upregulation or GALNT7 silencing to alter the secretion of immunomodulatory molecules by melanoma cells. For that, CD4+ splenocytes isolated from *FoxP3*-GFP mice (Bettelli et al., 2006) were activated ex vivo with CD28 and CD3 antibodies and then incubated in the presence of supernatants from scrambled, *miR-30d*, or siGALNT7-transfected A375 melanoma cells. We observed that supernatants from *miR-30d* or siGALNT7 cells display increased ability to suppress T cell activation (assessed by expression of surface markers CD25 and CD69) (Figure 8A), and total T cell number (Figure 8B) than those from scrambled-transfected cells. Importantly, these effects of *miR-30d* were reversed by coexpression of GALNT7 cDNA in 5B1 melanoma cells (Figures 8C and 8D). In addition, supernatants from *miR-30d* and siGALNT7 promoted T cell differentiation into Tregs, as indicated by the number of CD25+ GFP+ (Foxp3+) cells (Figure S7C). Moreover, we found that concomitant silencing of IL-10 by siRNA only partially counteracted *miR-30d*'s immunosuppressive activities (Figures 8A and 8B; Figure S7C). Therefore, our data suggest that IL-10 is one of multiple immunomodulatory molecules in *miR-30d*'s regulated cellular secretome.

DISCUSSION

We have demonstrated that *miR-30d/30b* overexpression enhances the invasive capacity of melanoma cells in vitro and increases their metastatic potential in vivo, predominantly by suppressing GALNT7. Downregulation of *miR-30d* produced the opposite effects, whereas direct silencing of GALNT7 replicated most effects of *miR-30d/b* overexpression. Changes in glycosylation patterns have been associated with tumor progression for some time (Dennis et al., 1999), yet the specific molecular mechanisms underlying abnormal glycosylation and the downstream processes directly or indirectly contributing to metastasis remain poorly characterized. Strikingly, aberrant miRNA-mediated regulation of a GalNAc-T promoted both cell motility and immunosuppressive mechanisms, which could synergize during metastasis.

Glycosylation in Tumor Progression

Our lectin arrays revealed that GALNT7 silencing or *miR-30d* upregulation has specific effects on O-glycans and, to a lesser

extent, on N-glycosylated substrates. Alterations in O-glycans have many biological consequences in cancer because potential ligands responsible for interactions between cancer cells and their microenvironment are changed. This influences the growth and survival of the cell and its interactions with lectins and cell surface receptors on neighboring cells or immune cells, all of which are important for its ability to metastasize (Brockhausen, 2006). GalNAc-Ts initiate mucin-type O-linked glycosylation in the Golgi apparatus by catalyzing the transfer of GalNAc to serine and threonine residues on target proteins (Ten Hagen et al., 2003). GalNAc-Ts have different but overlapping substrate specificities and patterns of expression. Our glycomic analysis revealed that GALNT7 silencing has broad effects on the glycosylation of melanoma cells beyond its known transferase activity. These effects could be modulated through mislocalization of other enzymes in the pathway due to loss of the transferase or alterations in protein localization and stability that influence the general glycosylation phenotype. Regardless, the glycomic signature is clearly rescued by overexpression of GALNT7, indicating that the effects are specific to this enzyme. This modified glycocode might, at least partially, account for *miR-30d*/siGALNT7 phenotype, even though the direct effectors (i.e., proteoglycans, signaling pathways) of their proinvasive and immunomodulatory actions could not be elucidated at this time. Preincubation with PTX did not affect *miR-30d*'s prometastatic effects, suggesting that Gi-dependent chemokine signaling is not a key player, at least under those experimental conditions.

We have shown that expression of GALNT7 and GALNT1 is controlled by *miR-30b/30d* levels, which increase during melanoma tumor progression in parallel with advancing stage and metastatic potential at the time of diagnosis. Intriguingly, in addition to GALNT1 and GALNT7, other GalNAc-T family members carry *miR-30d* recognition sites. We found that the expression of many of them inversely correlated with *miR-30d* levels in human samples, suggesting that this miRNA might coordinately regulate the entire GALNT family. Not much is known about the regulation of the GALNT family, though another miRNA, miR-378, with a potential effect in osteoblast differentiation, was shown to modulate GALNT7 (Kahai et al., 2009).

It is interesting to note that a prometastatic role for *miR-30d* has also been recently shown in hepatocellular carcinoma (Yao et al., 2010), and that *miR-30d* levels in the sera of patients with lung cancer correlate with poor prognosis (Hu et al., 2010). Together, these studies indicate that this miRNA cluster (and possibly GALNT suppression) might exert a common prometastatic effect in various cancers. Thus, the pleiotropic effects (immunosuppressive and proinvasive) of *miR-30d* described here for melanoma—mostly mediated by GalNAc-T suppression—might be relevant in other tumor types. In fact, metastatic clones derived from colorectal cancer cells have altered expression of various GalNAc-Ts in comparison with their nonmetastatic parental counterparts (Kato et al., 2010).

Curiously, miR-30e, which shares a seed region with *miR-30b/d* but is located in a separate genomic location, has shown an antimetastatic role in breast cancer (Yu et al., 2010). A plausible explanation for this apparent paradox is that whereas O-glycosylation of specific substrates, particularly of mucins, promotes breast or colon cancer progression (Brockhausen, 2006), the expression of mucins and their contribution to metastasis in melanoma are known to be limited (Bhavanandan, 1991). In addition the cell type-specific repertoire of GalNAc-Ts, which vary with cellular differentiation and malignant transformation (Mandel et al., 1999), could account for the opposing outcomes of miR-30e and *miR-30b/30d* induction in different tumors. These observations underscore the context-dependence of miRNA functions in cancer.

Although the prometastatic action of *miR-30d* is critically mediated by GALNT7 silencing, we observed that GALNT7 ectopic expression did not completely counteract *miR-30d*'s effects in vivo, suggesting a contribution of other *miR-30d* targets. In fact, in addition to the GALNT family, we validated other *miR-30d* targets such as SEMA3A, which exerts antiangiogenic functions (Maione et al., 2009; Serini et al., 2003), and *CESLR3* and *TWF1*, which are involved in cell-to-cell interactions and migration. However, downregulation of these genes failed to promote melanoma cell invasion through a fibronectin coat. Nevertheless, they may mediate other metastatic abilities not tested here, such as vascularization, adhesion, or motility. The contributions of SEMA3A, CESLR3, and TWF1 to *miR-30b/30d* prometastatic function need to be further investigated.

Immune Modulation in Melanoma

Melanoma is a paradigmatically immunogenic tumor, with abundant inflammatory infiltrates in both cutaneous and metastatic lesions, yet it manages to evade this upregulated host immune response (Lee et al., 2005; Real et al., 2001; Redondo et al., 2003). We found that *miR-30d* overexpression correlates with reduced CD3+ T cell recruitment and accumulation of Tregs at the metastatic site in vivo. Consistently, we demonstrated that *miR-30d* upregulation alters melanoma cells' secretome such that it suppresses T cell activation and favors Treg induction ex vivo. These effects can be partially mediated by increased IL-10 secretion, which results from GALNT7 suppression. This *miR-30b/30d*-GALNT7-IL-10 axis could provide a mechanistic explanation for the immunosuppressive behavior of some metastatic melanomas. We observed some association between higher *miR-30d* expression and more FOXP3-positive lymphocytes (putative Tregs) in human metastatic samples. Surprisingly, high *30d* levels significantly correlated with FOXP3 expression in the tumor cells themselves. The expression of FOXP3 by tumor cells was already reported in several cancer types (Hinz et al., 2007; Merlo et al., 2009), including melanoma (Ebert et al., 2008). It has been proposed that tumor cells expressing FOXP3 share immunosuppressive effects with Tregs (Martin et al., 2010), which might represent a new mechanism of immune evasion in melanoma. Both cell and non-cell autonomous mechanisms, potentially exerted by *miR-30d*, could cooperate to restrain the host antitumoral response. *miR-30d* prometastatic effects, critically mediated by GALNT7 suppression, are prominent even in the absence of a functional host immune system, as indicated by our experiments conducted in NOG/SCID mice. However, our results in immunocompetent mice reveal notable immunosuppressive effects associated with *miR-30d* upregulation, which might synergize with its proinvasive properties during metastasis.

The control of immunostimulant or immunosuppressive molecules by miRNAs in the context of tumor formation and progression is largely unexplored. miR-21, a miRNA with established

tumorigenic role (Esquela-Kerscher and Slack, 2006), has been shown to negatively regulate TLR4 via targeting the proinflammatory tumor suppressor PDCD4 (Sheedy et al., 2010), but to our knowledge, the contribution of this mechanism to the tumorigenic activities of miR-21 remains unknown. Evidence of another miRNA directly targeting IL-10, miR-106a, has been recently reported (Sharma et al., 2009). It is interesting to note in this context that we found reduced miR-106a levels in *miR-30d*-transduced cells (data not shown), which suggests a possible miRNA network converging on the modulation of IL-10 levels.

A recent report showed that Snail-mediated induction of epithelial to mesenchymal transition induces an immunosuppressive response in melanoma cells mainly by inducing the cytokine TSP1 (Kudo-Saito et al., 2009). These data and our current results reveal that cell migration and immune evasion are intimately connected during metastasis, and our findings suggest that GalNAc-Ts can serve as a link between the two.

In sum this study shows that a single miRNA can exert both proinvasive and immunomodulatory effects, and that both actions could be critically mediated by one target, GALNT7. Our data could have important prognostic implications: higher *miR-30d* expression correlates with advanced melanoma and aggressive biological behavior, and is a predictor of time to death with melanoma, independent of thickness. Moreover, *miR-30d* targeting represents a plausible therapeutic approach: targeting *miR-30d* in tumor cells with chemically modified oligonucleotides or artificial decoys (reviewed in Tong and Nemunaitis, 2008; Valastyan and Weinberg, 2009) could derepress the endogenous GALNT7 levels, simultaneously counteracting both its proinvasive and immunosuppressive effects. More research is needed to understand the effects of concurrently derepressing other *miR-30d* targets, but the possibility remains that miRNA targeting could synergistically impede metastasis as much as miRNA upregulation promotes it.

EXPERIMENTAL PROCEDURES

Cell Lines

Cell lines were cultured as previously described (Segura et al., 2009; Cruz-Munoz et al., 2008). HEK293T and A375 cells were purchased from American Type Culture Collection (ATCC). The B16F10 mouse melanoma cell line and the human WM35 and WM98 cell lines were acquired from the Wistar Institute. Cell lines 4L and 5B1 were isolated and cultured as previously described (Cruz-Munoz et al., 2008). 4L, 5B1, A375, and B16F10 are metastatic melanoma cell lines, whereas WM35 and WM98 were derived from primary melanomas.

Luciferase Assays

HEK293T cells were seeded into 96-well plates and cotransfected with 3′UTR vectors and indicated amounts of *miR-30b* or *-30d* mimics or miRIDIAN mimic negative control (Dharmacon). Luciferase activity was measured using the Dual-Glo Luciferase Assay System (Promega). *Renilla* luciferase activity was normalized to corresponding firefly luciferase activity and plotted as a percentage of the control.

Ex Vivo T Cell Activation, Followed by FACS Analysis

CD4+ splenocytes were isolated from *Foxp3*-GFP mice using a CD4+ T Cell Isolation Kit (Miltenyi Biotec). A total of 1×10^6 cells/24 wells were then incubated in conditioned media of melanoma cells supplemented with 25 μl of Dynabeads Human CD3/CD28 T-Cell Activator (Invitrogen). FACS analysis was performed after 72 hr on cells stained for CD4 (APC-Cy7-conjugated; BioLegend), CD25 (APC-conjugated; eBioscience), and CD69 (PE-conjugated; BD Biosciences).

Clinical Specimens

Human melanoma specimens (primary, metastatic) were collected at the time of surgery. Approval to collect specimens was granted by New York University Institutional Review Board protocol number 10362, "Development of an NYU Interdisciplinary Melanoma Cooperative Group: A clinicopathological database." Informed consent was obtained from all subjects included.

Mouse Experiments

Experiments were conducted following protocols approved by the NYU Institutional Animal Care Use Committee (IACUC) (protocol number 080109).

Statistical Methodologies

Statistical significance was determined by paired or unpaired Student's t test in cases of standardized expression data. One-way ANOVA was performed for multiple group comparisons (GraphPad Prism Software). Wilcoxon matched pairs test and Mann-Whitney U tests for nonparametric analyses of non-Gaussian data. Chi-square test and McNemar's test were used for testing association among unmatched and matched categorical variables. In particular, chi-square test and Fisher's exact test were used to assess association of *miR-30d* with FOXP3 staining in T cells and in melanoma cells (Figure S7A). Multivariable COX PH models were used to analyze time-to-recurrence and overall survival when adjusted for primary tumor thickness and ulceration status. Log rank test was used for analyses presented in Figures 1E and 1F.

ACCESSION NUMBERS

Coordinates have been deposited in the GEOArchive with accession code GSE27718.

SUPPLEMENTAL INFORMATION

Supplemental Information includes Supplemental Experimental Procedures, seven figures, and two tables and can be found with this article online at doi:10.1016/j.ccr.2011.05.027.

ACKNOWLEDGMENTS

We thank members of the NYU Cancer Institute Genomics Facility for array analysis, and Dr. Cindy Loomis and members of the NYU Cancer Institute Histopathology and Immunohistochemistry Core Laboratories for tissue processing and histological stainings. We thank Drs. Dan Littman and Vijay Kuchroo for the *FoxP3*-GFP mice. We are grateful to Elisa De Stanchina (MSKCC), Silvia Menendez, and Lisa Koetz for technical assistance, Chin-Siean Tay for IF stainings, and to Dr. Michelle Krogsgaard and members of her lab for discussions and technical assistance. This work was funded by the ConCerN Foundation, the Melanoma Research Foundation, the Marc Jacobs Campaign, and funds from the NIH-NCI Cancer Center Support Grant P30CA016087. L.K.M. is supported by a NIH 7 DP2 OD004711-02 grant. M.F.S. is supported by a National Cancer Center fellowship, and R.D.M. by an EMBO post-doctoral fellowship. The authors declare no conflict of interest.

Received: July 27, 2010
Revised: February 25, 2011
Accepted: May 26, 2011
Published: July 11, 2011

REFERENCES

Bettelli, E., Carrier, Y., Gao, W., Korn, T., Strom, T.B., Oukka, M., Weiner, H.L., and Kuchroo, V.K. (2006). Reciprocal developmental pathways for the generation of pathogenic effector TH17 and regulatory T cells. Nature *441*, 235–238.

Bhavanandan, V.P. (1991). Cancer-associated mucins and mucin-type glycoproteins. Glycobiology *1*, 493–503.

Bogunovic, D., O'Neill, D.W., Belitskaya-Levy, I., Vacic, V., Yu, Y.L., Adams, S., Darvishian, F., Berman, R., Shapiro, R., Pavlick, A.C., et al. (2009). Immune profile and mitotic index of metastatic melanoma lesions enhance clinical staging in predicting patient survival. Proc. Natl. Acad. Sci. USA *106*, 20429–20434.

Brockhausen, I. (2006). Mucin-type O-glycans in human colon and breast cancer: glycodynamics and functions. EMBO Rep. *7*, 599–604.

Calin, G.A., and Croce, C.M. (2006). MicroRNA signatures in human cancers. Nat. Rev. Cancer *6*, 857–866.

Croce, C.M., and Calin, G.A. (2005). miRNAs, cancer, and stem cell division. Cell *122*, 6–7.

Cruz-Munoz, W., Man, S., Xu, P., and Kerbel, R.S. (2008). Development of a preclinical model of spontaneous human melanoma central nervous system metastasis. Cancer Res. *68*, 4500–4505.

Dennis, J.W., Granovsky, M., and Warren, C.E. (1999). Glycoprotein glycosylation and cancer progression. Biochim. Biophys. Acta *1473*, 21–34.

Ebert, L.M., Tan, B.S., Browning, J., Svobodova, S., Russell, S.E., Kirkpatrick, N., Gedye, C., Moss, D., Ng, S.P., MacGregor, D., et al. (2008). The regulatory T cell-associated transcription factor FoxP3 is expressed by tumor cells. Cancer Res. *68*, 3001–3009.

Ehlers, J.P., Worley, L., Onken, M.D., and Harbour, J.W. (2005). DDEF1 is located in an amplified region of chromosome 8q and is overexpressed in uveal melanoma. Clin. Cancer Res. *11*, 3609–3613.

Esquela-Kerscher, A., and Slack, F.J. (2006). Oncomirs—microRNAs with a role in cancer. Nat. Rev. Cancer *6*, 259–269.

Gupta, G.P., and Massagué, J. (2006). Cancer metastasis: building a framework. Cell *127*, 679–695.

Gupta, P.B., Mani, S., Yang, J., Hartwell, K., and Weinberg, R.A. (2005). The evolving portrait of cancer metastasis. Cold Spring Harb. Symp. Quant. Biol. *70*, 291–297.

Hinz, S., Pagerols-Raluy, L., Oberg, H.H., Ammerpohl, O., Grüssel, S., Sipos, B., Grützmann, R., Pilarsky, C., Ungefroren, H., Saeger, H.D., et al. (2007). Foxp3 expression in pancreatic carcinoma cells as a novel mechanism of immune evasion in cancer. Cancer Res. *67*, 8344–8350.

Hu, Z., Chen, X., Zhao, Y., Tian, T., Jin, G., Shu, Y., Chen, Y., Xu, L., Zen, K., Zhang, C., and Shen, H. (2010). Serum microRNA signatures identified in a genome-wide serum microRNA expression profiling predict survival of non-small-cell lung cancer. J. Clin. Oncol. *28*, 1721–1726.

Kahai, S., Lee, S.C., Lee, D.Y., Yang, J., Li, M., Wang, C.H., Jiang, Z., Zhang, Y., Peng, C., and Yang, B.B. (2009). MicroRNA miR-378 regulates nephronectin expression modulating osteoblast differentiation by targeting GalNT-7. PLoS One *4*, e7535.

Kato, K., Takeuchi, H., Kanoh, A., Miyahara, N., Nemoto-Sasaki, Y., Morimoto-Tomita, M., Matsubara, A., Ohashi, Y., Waki, M., Usami, K., et al. (2010). Loss of UDP-GalNAc:polypeptide N-acetylgalactosaminyltransferase 3 and reduced O-glycosylation in colon carcinoma cells selected for hepatic metastasis. Glycoconj. J. *27*, 267–276.

Krishnamoorthy, L., Bess, J.W., Jr., Preston, A.B., Nagashima, K., and Mahal, L.K. (2009). HIV-1 and microvesicles from T cells share a common glycome, arguing for a common origin. Nat. Chem. Biol. *5*, 244–250.

Kudo-Saito, C., Shirako, H., Takeuchi, T., and Kawakami, Y. (2009). Cancer metastasis is accelerated through immunosuppression during Snail-induced EMT of cancer cells. Cancer Cell *15*, 195–206.

Lee, J.H., Torisu-Itakara, H., Cochran, A.J., Kadison, A., Huynh, Y., Morton, D.L., and Essner, R. (2005). Quantitative analysis of melanoma-induced cytokine-mediated immunosuppression in melanoma sentinel nodes. Clin. Cancer Res. *11*, 107–112.

Lewis, B.P., Burge, C.B., and Bartel, D.P. (2005). Conserved seed pairing, often flanked by adenosines, indicates that thousands of human genes are microRNA targets. Cell *120*, 15–20.

Lu, Y., Ryan, S.L., Elliott, D.J., Bignell, G.R., Futreal, P.A., Ellison, D.W., Bailey, S., and Clifford, S.C. (2009). Amplification and overexpression of Hsa-miR-30b, Hsa-miR-30d and KHDRBS3 at 8q24.22-q24.23 in medulloblastoma. PLoS One *4*, e6159.

Ma, L., Teruya-Feldstein, J., and Weinberg, R.A. (2007). Tumour invasion and metastasis initiated by microRNA-10b in breast cancer. Nature *449*, 682–688.

Ma, L., Young, J., Prabhala, H., Pan, E., Mestdagh, P., Muth, D., Teruya-Feldstein, J., Reinhardt, F., Onder, T.T., Valastyan, S., et al. (2010). miR-9, a MYC/MYCN-activated microRNA, regulates E-cadherin and cancer metastasis. Nat. Cell Biol. *12*, 247–256.

Maione, F., Molla, F., Meda, C., Latini, R., Zentilin, L., Giacca, M., Seano, G., Serini, G., Bussolino, F., and Giraudo, E. (2009). Semaphorin 3A is an endogenous angiogenesis inhibitor that blocks tumor growth and normalizes tumor vasculature in transgenic mouse models. J. Clin. Invest. *119*, 3356–3372.

Mandel, U., Hassan, H., Therkildsen, M.H., Rygaard, J., Jakobsen, M.H., Juhl, B.R., Dabelsteen, E., and Clausen, H. (1999). Expression of polypeptide GalNAc-transferases in stratified epithelia and squamous cell carcinomas: immunohistological evaluation using monoclonal antibodies to three members of the GalNAc-transferase family. Glycobiology *9*, 43–52.

Martin, F., Ladoire, S., Mignot, G., Apetoh, L., and Ghiringhelli, F. (2010). Human FOXP3 and cancer. Oncogene *29*, 4121–4129.

Merlo, A., Casalini, P., Carcangiu, M.L., Malventano, C., Triulzi, T., Mènard, S., Tagliabue, E., and Balsari, A. (2009). FOXP3 expression and overall survival in breast cancer. J. Clin. Oncol. *27*, 1746–1752.

Palmgren, S., Vartiainen, M., and Lappalainen, P. (2002). Twinfilin, a molecular mailman for actin monomers. J. Cell Sci. *115*, 881–886.

Pilobello, K.T., Krishnamoorthy, L., Slawek, D., and Mahal, L.K. (2005). Development of a lectin microarray for the rapid analysis of protein glycopatterns. Chembiochem *6*, 985–989.

Real, L.M., Jimenez, P., Kirkin, A., Serrano, A., García, A., Cantón, J., Zeuthen, J., Garrido, F., and Ruiz-Cabello, F. (2001). Multiple mechanisms of immune evasion can coexist in melanoma tumor cell lines derived from the same patient. Cancer Immunol. Immunother. *49*, 621–628.

Redondo, P., Sánchez-Carpintero, I., Bauzá, A., Idoate, M., Solano, T., and Mihm, M.C., Jr. (2003). Immunologic escape and angiogenesis in human malignant melanoma. J. Am. Acad. Dermatol. *49*, 255–263.

Scheel, C., Onder, T., Karnoub, A., and Weinberg, R.A. (2007). Adaptation versus selection: the origins of metastatic behavior. Cancer Res. *67*, 11476–11479.

Segura, M.F., Hanniford, D., Menendez, S., Reavie, L., Zou, X., Alvarez-Diaz, S., Zakrzewski, J., Blochin, E., Rose, A., Bogunovic, D., et al. (2009). Aberrant miR-182 expression promotes melanoma metastasis by repressing FOXO3 and microphthalmia-associated transcription factor. Proc. Natl. Acad. Sci. USA *106*, 1814–1819.

Segura, M.F., Belitskaya-Lévy, I., Rose, A.E., Zakrzewski, J., Gaziel, A., Hanniford, D., Darvishian, F., Berman, R.S., Shapiro, R.L., Pavlick, A.C., et al. (2010). Melanoma MicroRNA signature predicts post-recurrence survival. Clin. Cancer Res. *16*, 1577–1586.

Serini, G., Valdembri, D., Zanivan, S., Morterra, G., Burkhardt, C., Caccavari, F., Zammataro, L., Primo, L., Tamagnone, L., Logan, M., et al. (2003). Class 3 semaphorins control vascular morphogenesis by inhibiting integrin function. Nature *424*, 391–397.

Sharma, A., Kumar, M., Aich, J., Hariharan, M., Brahmachari, S.K., Agrawal, A., and Ghosh, B. (2009). Posttranscriptional regulation of interleukin-10 expression by hsa-miR-106a. Proc. Natl. Acad. Sci. USA *106*, 5761–5766.

Sheedy, F.J., Palsson-McDermott, E., Hennessy, E.J., Martin, C., O'Leary, J.J., Ruan, Q., Johnson, D.S., Chen, Y., and O'Neill, L.A. (2010). Negative regulation of TLR4 via targeting of the proinflammatory tumor suppressor PDCD4 by the microRNA miR-21. Nat. Immunol. *11*, 141–147.

Talmadge, J.E. (2007). Clonal selection of metastasis within the life history of a tumor. Cancer Res. *67*, 11471–11475.

Tavazoie, S.F., Alarcón, C., Oskarsson, T., Padua, D., Wang, Q., Bos, P.D., Gerald, W.L., and Massagué, J. (2008). Endogenous human microRNAs that suppress breast cancer metastasis. Nature *451*, 147–152.

Ten Hagen, K.G., Fritz, T.A., and Tabak, L.A. (2003). All in the family: the UDP-GalNAc:polypeptide N-acetylgalactosaminyltransferases. Glycobiology *13*, 1R–16R.

Tong, A.W., and Nemunaitis, J. (2008). Modulation of miRNA activity in human cancer: a new paradigm for cancer gene therapy? Cancer Gene Ther. *15*, 341–355.

Valastyan, S., and Weinberg, R.A. (2009). Assaying microRNA loss-of-function phenotypes in mammalian cells: emerging tools and their potential therapeutic utility. RNA Biol. *6*, 541–545.

Van Den Berg, C., Guan, X.-Y., Von Hoff, D., Jenkins, R., Bittner, M., Griffin, C., Kallioniemi, O., Visakorpi, T., McGill, J., Herath, J., et al. (1995). DNA sequence amplification in human prostate cancer identified by chromosome microdissection: potential prognostic implications. Clin. Cancer Res. *1*, 11–18.

Visapää, H., Seligson, D., Eeva, M., Gaber, F., Rao, J., Belldegrun, A., and Palotie, A. (2003). 8q24 amplification in transitional cell carcinoma of bladder. Appl. Immunohistochem. Mol. Morphol. *11*, 33–36.

Wu, Q., and Maniatis, T. (1999). A striking organization of a large family of human neural cadherin-like cell adhesion genes. Cell *97*, 779–790.

Yao, J., Liang, L., Huang, S., Ding, J., Tan, N., Zhao, Y., Yan, M., Ge, C., Zhang, Z., Chen, T., et al. (2010). MicroRNA-30d promotes tumor invasion and metastasis by targeting Galphai2 in hepatocellular carcinoma. Hepatology *51*, 846–856.

Yu, F., Deng, H., Yao, H., Liu, Q., Su, F., and Song, E. (2010). Mir-30 reduction maintains self-renewal and inhibits apoptosis in breast tumor-initiating cells. Oncogene *29*, 4194–4204.

Yu, H., Pardoll, D., and Jove, R. (2009). STATs in cancer inflammation and immunity: a leading role for STAT3. Nat. Rev. Cancer *9*, 798–809.